WATER RESOURCES RESEARCH, VOL. 35, NO. 11, PAGES 3303–3313, NOVEMBER 1999

The effect of water content on solute transport in unsaturated porous media

Ingrid Y. Padilla, T.-C. Jim Yeh, and Martha H. Conklin

Department of Hydrology and Water Resources, University of Arizona, Tucson

Abstract. The effect of water content on NaCl transport in unsaturated porous media was investigated under steady state flow conditions for water contents ranging between full saturation and 15% by volume. The experiments were conducted in a 25 cm column packed with homogeneous sand. Results of the experiments indicate that solute transport in unsaturated porous media is subject to greater velocity variations and slower solute mixing than one in saturated media. As a result, NaCl breakthrough curves (BTCs) show earlier initial arrival and greater tailing and variance as the average water content decreases. These results suggest that transport processes in our experiments have not fully developed to the Fickian regime at lower water contents. Because the classical convection-dispersion equation does not adequately describe the movement of solutes under the pre-Fickian regime, a mobile-immobile model was employed to reproduce the BTCs obtained under unsaturated conditions. In general, the results indicate that at lower water contents the medium has a greater fraction of immobile water, higher dispersion, and slower mass transfer between the mobile and immobile regions. A power law relationship between dispersion and water content–normalized velocities was found to exist for our experiments and other experiments reported in the literature using different porous media. Thus we suggest dispersivity is not only a function of properties of the media but also of water content.

1. Introduction

In classical groundwater hydrology the velocity of solutes moving through unsaturated porous media is commonly defined as the average velocity for all flow paths over a representative elementary volume (REV). This average velocity therefore does not describe velocity variations caused by heterogeneities at scales smaller than the REV. The effect of these velocity variations on solute transport has generally been incorporated in the transport equation using the concept of hydrodynamic dispersion. That is, deviations in concentration fluxes resulting from velocity variations are expressed as a dispersive flux. Analogous to the classical representation of molecular diffusion process, Fick's law is employed to relate this flux to the concentration gradient $\partial C/\partial z$, where C is the solute concentration and z is the spatial coordinate. For one-dimensional solute transport in homogeneous isotropic porous media under steady flow with a uniform water content and constant velocity the governing equation can be written as

$$R\frac{\partial C}{\partial t} = D\frac{\partial^2 C}{\partial z^2} - v\frac{\partial C}{\partial z}. \tag{1}$$

Equation (1) is often referred to as the convection-dispersion equation (CDE), in which v is pore water velocity ($v = q/\theta$, where q is the Darcy flux and θ is volumetric water content), t is time, and R is the retardation coefficient accounting for equilibrium linear sorption processes. The hydrodynamic dispersion coefficient D is often defined as the sum of effective molecular diffusion $D_w\tau_w$ and mechanical dispersion D_h:

$$D = D_w\tau_w + D_h \qquad D_h = \eta v^n, \tag{2}$$

Paper number 1999WR900171.
0043-1397/99/1999WR900171$09.00

where D_w is the diffusion coefficient in bulk water, τ_w is a tortuosity factor, η is dispersivity, and n is an empirical coefficient. The tortuosity factor is thought to account for the shape and length of the molecular path and depends on water content but not on velocity [*Nielsen et al*., 1986]. The dispersivity is generally considered to be an intrinsic property of porous media under fully saturated conditions; however, greater values have been reported for the same media when unsaturated flow conditions are imposed in the system [*De Smedt et al*., 1986; *Maraqa et al*., 1997; *Matsubayashi et al*., 1997]. The constant n has been found to range between 1 and 2 [*Bear*, 1972].

It has generally been accepted that the CDE is the fundamental equation for describing transport of solutes in porous media [e.g., *Bear*, 1972]. This equation, however, is valid only when the transport of a solute has reached the Fickian regime in which the rate of solute spread grows linearly with time [*Fischer et al*., 1979] and the dispersive flux becomes linearly proportional to the concentration gradient. The Fickian regime occurs only after sufficient "forgetting" time has elapsed (i.e., the solute has been able to sample the whole field of velocities and the solute velocity is independent of its initial velocity). This means that a solute plume must travel over a large distance, or for a long enough time, to interact with many small-scale heterogeneities of the porous medium before the CDE can be applied. For solute transport in a uniformly packed sand column under fully saturated conditions the distance is of the order of several thousands of sand grains [*Yeh*, 1998], which is much smaller than the length of a sand column in general. As a consequence, this requirement is often satisfied, and the CDE is considered adequate for the analysis of solute transport in the sand column under fully saturated conditions. However, as the sand column desaturates, the number

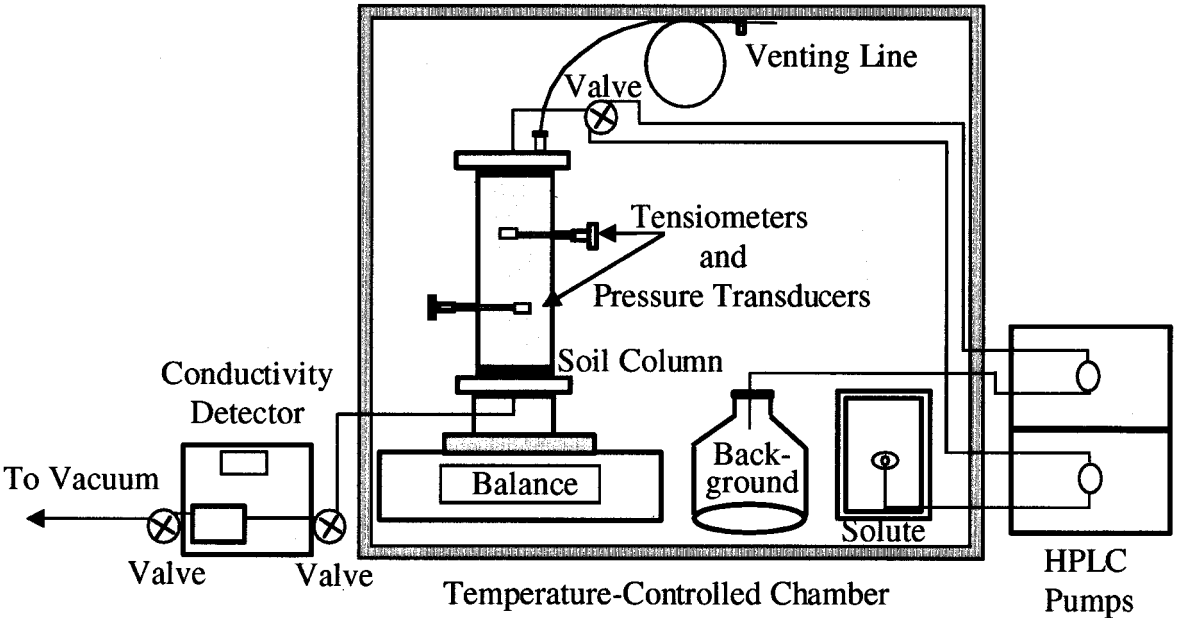

Figure 1. Experimental apparatus for transport experiments in unsaturated porous media.

of flow paths decreases, and velocity variations increase. A solute plume in an unsaturated sand column must then travel a greater distance to attain complete mixing and to reach the Fickian regime than one in a saturated column. In many cases this distance may greatly exceed the length of the column. As a result, solute breakthrough is often characterized by multiple peaks, early initial arrival, and long effluent tailings that cannot be adequately described by the CDE [*Yeh*, 1998].

In the absence of a theoretical framework to define the relationship between dispersive flux and concentration gradient for the pre-Fickian regime many researchers have used the dead-end pore model [*Coats and Smith*, 1964] to describe the transport of solutes exhibiting long effluent tailing in laboratory experiments. A similar conceptual model, the mobile-immobile model (MIM), has also been applied to describe this solute transport behavior in unsaturated porous media [*Bond and Wierenga*, 1990; *De Smedt and Wierenga*, 1984; *Gaudet et al*., 1977; *van Genuchten and Wierenga*, 1976]. The approach leads to a two-region convection-dispersion equation with a first-order solute exchange process between the mobile and immobile regions [*van Genuchten and Wierenga*, 1976; *Wierenga and van Genuchten*, 1989]:

$$\theta_m R_m \frac{\partial C_m}{\partial t} + \theta_{im} R_{im} \frac{\partial C_{im}}{\partial t} = \theta_m D_m \frac{\partial^2 C_m}{\partial z^2} - \theta_m v_m \frac{\partial C_m}{\partial z} \tag{3a}$$

$$\theta_{im} R_{im} \frac{\partial C_{im}}{\partial t} = \alpha (C_m - C_{im}), \tag{3b}$$

where the subscripts m and im refer to mobile and immobile liquid phases, respectively, $D_m = D_h/\beta = (D - D_w\tau_w)/\beta$ (where β is the mobile water fraction θ_m/θ), v_m is mobile pore water velocity (where $v_m = q/\theta_m$), and α is a first-order mass transfer coefficient that accounts for diffusion between the mobile and immobile water regions. Values for θ_m and v_m are assumed constant in space and time. Values of β have been reported to decrease as water content decreases in unsaturated systems [*De Smedt and Wierenga*, 1984; *De Smedt et al*., 1986; *Gaudet et al*., 1977; *van Genuchten and Wierenga*, 1976]. The mass transfer coefficient has been related to the interfacial area between the two regions, volume and geometry of the immobile water, and velocity [e.g., *Armstrong et al*., 1994; *Bajracharya and Barry*, 1997; *De Smedt and Wierenga*, 1984; *Rao et al*., 1980a, b; *van Genuchten and Wierenga*, 1977]. Notice that if $\theta_{im} = 0$, equation (3) reduces to the CDE (equation (1)) and will be referred to as the CDE equilibrium model; otherwise, it is referred to as the nonequilibrium or MIM model.

Few laboratory experiments have attempted to investigate systematically solute transport through porous media under various degrees of saturation, although numerous experiments have been conducted in the past to study solute transport in unsaturated porous media. Furthermore, little attention has been given to the validity of Fick's law in unsaturated porous media under different water contents. Therefore the objective of this study was to explore experimentally the effect of water contents on the solute transport in unsaturated porous media.

2. Experimental Setup, Materials, and Methods

The experimental setup used in this study is illustrated in Figure 1. The system includes a stainless steel (SS) column, 4.78 cm ID and 25 cm long, packed with silica sand. SS porous plates (Mott Metallurgical) with average pore diameters of 100 and 0.5 μm were placed at the top and bottom ends of the column, respectively. Two tensiometers with SS porous cups (1.52 cm long, 0.48 cm OD, and average pore diameter of 2 μm) were mounted on opposite sides of the column at 7.5 cm from each column end. The tensiometers were connected to pressure transducers (Micro Switch 236PC-15GW) to monitor soil-water tension within the column. The inlet of the column was connected to high-performance liquid chromatography (HPLC) pumps (SSI Acuflow Series II Pump), which delivered the liquid phase at constant flow rates. A venting port was placed near the inlet to allow the movement of air in and out of the column while establishing water flow equilibrium. The column was placed vertically on a top-loading balance (Mettler

Table 1. Experimental Conditions and Moment Analysis of Breakthrough Data

	Measured Parameters					Moment Analysis of Breakthrough Data			
Run	Q, $cm^3\ min^{-1}$	θ, $cm^3\ cm^{-3}$	v,[a] $cm\ min^{-1}$	$\Delta P/\Delta z$[b]	Pulse,[c] T	θ_e, $cm^3\ cm^{-3}$	v,[d] $cm\ min^{-1}$	σ min^2	Skewness, $min^{3/2}$
Saturated									
NC 20	1.031	0.45	0.128	−0.913	1.524	0.46	0.126	228	6.7
NC 21	1.032	0.45	0.129	−0.863	1.513	0.46	0.126	357	5.00
NC 23	0.264	0.45	0.033	−0.796	1.419	0.46	0.032	—	—
Unsaturated									
NaCl 1	1.030	0.31	0.184	−0.626	2.191	0.32	0.183	868	4.35
NaCl 2	1.038	0.31	0.188	−0.575	2.231	0.31	0.186	950	5.63
NaCl 3	1.028	0.32	0.182	−0.739	2.174	0.32	0.181	866	5.65
NaCl 4	0.775	0.20	0.214	0.017	2.587	0.20	0.215	939	3.16
NaCl 5	0.525	0.18	0.164	−0.059	2.647	0.18	0.157	8102	8.04
NaCl 6	0.313	0.16	0.107	−0.160	4.245	0.16	0.107	4536	1.97
NaCl 7	0.209	0.15	0.078	−0.097	5.422	0.15	0.075	66043	16.95
NaCl 8	0.523	0.19	0.151	−0.185	4.181	0.20	0.145	1132	1.71
NaCl 9	0.895	0.24	0.206	−0.677	3.219	0.26	0.192	3025	10.04
NaCl 10	0.771	0.22	0.196	−0.446	4.493	0.23	0.187	861	7.96
NaCl 12	0.312	0.18	0.095	−0.050	5.025	0.18	0.095	8261	1.17
NaCl 21	1.043	0.27	0.213	−0.189	3.476	0.29	0.202	3950	12.19
NaCl 22	0.887	0.25	0.201	−0.067	4.861	0.25	0.193	4236	13.40

[a] Pore water velocity determined from volumetric flow rates, column cross-sectional area, and water contents.
[b] In cm $H_2O\ cm^{-1}$, where the reference elevation ($z = 0$) is the bottom of the column and the gradient is calculated in the direction of flow.
[c] In pore volumes ($T = t_p v/L$), where t_p is the step duration time.
[d] Pore water velocity determined from mean arrival time of the NaCl center of mass.

PM 6100), and the outlet was connected to a vacuum chamber. The balance was used to monitor the average water content of the column throughout the experiments. The vacuum chamber established a constant head boundary for water flow at the column bottom and achieved specific soil-water tensions and water contents in the sand for given water flow rates. Effluent solute concentrations were monitored throughout time using a flow-through conductivity detector (Wescan Conductivity Detector, model 213).

The sand used in the column was primarily composed of quartz grains and contained very little organic carbon (fraction of organic carbon (foc) ~0.009%). A particle size distribution ranging between 53 and 425 μm with an average particle size of 250 μm was obtained by wet sieving the sand with purified water. The sand was fairly homogeneous and well sorted, with over 80% of the particles falling between 149 and 300 μm. Brunauer-Emmett-Teller (BET) analysis yielded a total specific surface area of 0.738 $m^2\ g^{-1}$ and an internal pore area of 0.112 $m^2\ g^{-1}$ [*Brunauer et al.*, 1938]. Although the external surface area contributed largely to the total specific surface area of the sand (~85%), the BET analysis reflected the presence of some internal porosity in the sand grains. Soil-water retention curves were determined using a "hanging column" procedure similar to that described by *Danielson and Sutherland* [1986] and *Klute* [1986] to determine the pore size distribution of porous media. Soil-water retention curves were analyzed using the parametric model of *van Genuchten* [1980],

$$S_w = \frac{\theta_w - \theta_r}{\theta_{sat} - \theta_r} = (1 + |\propto h|^{n_p})^{-m}, \quad (4)$$

where h is the soil-water tension, n_p and $\propto$ are shape parameters related to the pore size distribution, $m = 1 - 1/n_p$, θ_r is the residual water content, θ_{sat} is the saturated water content, and S_w represents the degree of water saturation. The measured soil-water retention curve for draining conditions is well represented by θ_r, α, and n_p values of 0.076, 0.027 cm^{-1}, and 4.74, respectively, showing a root-mean-square error of 0.0236 $cm^3_w\ cm^{-3}_{Total}$ on volumetric water content.

The column was uniformly packed to a dry bulk density of 1.49 g cm^{-3} and a total porosity of ~0.45 $cm^3\ cm^{-3}$. After packing, the column was saturated from the bottom with deaired solution. A pore volume of 204.5 cm^3 was measured by subtracting the column dry weight from that of the saturated column. This measurement suggested that the dead volume of the endcaps contributed <2% of the total pore volume of the media.

A total of 16 water-advecting transport experiments were conducted, three of which were performed under saturated flow conditions (Table 1). Prior to each experiment, steady state flow conditions were established using a background 2.0 mM aqueous NaCl solution. Unsaturated transport experiments were conducted by draining the column to specified water contents by lowering flow rates at the top of the column and/or adjusting the suction in the vacuum chamber. Once steady state flow rates, water contents, and soil-water tensions were reached, a 4.0 mM NaCl solution was introduced as a displacing fluid. The relatively similar solution concentrations were chosen to minimize any changes in hydraulic properties. The influent solution was switched back to the background solution after the NaCl concentration of the column effluent reached the inlet concentration C_0. Effluent concentrations were plotted versus time to establish the solute breakthrough curves (BTCs).

3. Data Analysis

The method of moments for temporal concentration distributions was used to characterize the NaCl breakthrough data. The absolute nth moment is defined as

$$M_n = \int_0^\infty t^n C(z, t)\, dt. \quad (5)$$

Experimental absolute moments M_n were obtained through numerical integration of the breakthrough data using the trapezoidal rule. The total mass of solute passing through the system was verified with the M_0 of the BTC. The first normalized absolute moment of the input pulse and the effluent concentration signal were used to estimate the mean arrival time of the center of NaCl mass (μ):

$$\mu = \frac{M_l^{\mathrm{II}}}{M_0^{\mathrm{II}}} - \frac{M_l^{\mathrm{I}}}{M_0^{\mathrm{I}}}, \tag{6}$$

where the I and II superscripts refer to the moments of the input and output signals, respectively. The mean arrival time was used in conjunction with the column length L to calculate the pore water velocity ($v = L/\mu$). An effective water content θ_e was then estimated from the Darcy flux divided by the moment-derived pore water velocity. Using normalized central moments,

$$M_n^* = \frac{\int_0^\infty \left(t - \frac{M_1}{M_0}\right)^n C(x, t)\, dt}{M_0}, \tag{7}$$

the variance of the breakthrough curve is calculated by

$$\sigma = M_2^{*\mathrm{II}} - M_2^{*\mathrm{I}} \tag{8}$$

In general, this variance represents the spread of the concentration distribution and is influenced by mechanical dispersion and molecular diffusion.

The influence of molecular diffusion on the spreading of the BTC data was evaluated by calculating the effective molecular diffusion where $D_w \sim 8 \times 10^{-4}$ cm^2 min^{-1} for NaCl [*Welty et al*., 1984] and τ_w was assumed to be linearly related to the degree of saturation of the media (S),

$$\tau_w = \tau_{\mathrm{sat}} \frac{S - S_r}{1 - S_r}, \tag{9}$$

where τ_{sat} is the tortuosity factor when the media is fully saturated and S_r is the "irreducible" saturation [*Burdine*, 1953]. A value of $\tau_{\mathrm{sat}} = 0.85$ was chosen as a representative value for sandy soil [*Ma and Selim*, 1994]. The value of $S_r = 0.17$ was obtained from soil-water retention curves of the sand used in these experiments.

The skewness of the BTC is a measure of the degree of asymmetry of the curve around its mean and is given by

$$\mathrm{SK} = \frac{M_3^*}{\sigma^{3/2}}. \tag{10}$$

A positive value of skewness signifies a distribution with an asymmetric tail extending out in time. For a conservative tracer the BTC is slightly skewed even though the transport process has reached the Fickian regime and fully conforms to the CDE. This skewness is attributable to the combined effect of convective and dispersive processes, similar to the physical concept of the Doppler effect. Any additional asymmetry of the solute concentration distribution may then reflect incomplete spatial averaging and non-Fickian transport processes.

Employing an approach similar to *Leij and Dane* [1992] and *Valocchi* [1985], the moments calculated for the NaCl breakthrough data were used to determine transport parameters for (3). The details of this approach are given by *Padilla* [1998]. For BTCs measured at the column outlet the retardation of the solute was estimated by the first moment.

In addition to the above moment analysis, a nonlinear least squares optimization code for estimating transport parameters, CXTFIT [*Toride et al*., 1995], was employed to estimate values of parameters in (1) and (3). For (1), two transport parameters (D and v) were estimated, while four transport parameters (v, D, α, and θ_m) were determined for (3). Pore water velocities were fitted to give more flexibility in the estimation procedure [*Toride et al*., 1995], and the retardation coefficient was fixed at 1.0 since the mean arrival time indicated that NaCl eluted at 1 pore volume. A first-type inlet condition was used since our experiments involved flux-averaged concentrations [*van Genuchten and Parker*, 1984]. A zero concentration gradient at infinity and an initial solute concentration C_I were assumed.

We recognize that the CXTFIT model assumes uniform velocity along a column. However, for some of our experiments the water content was nonuniform, and the velocity varied along the column (as indicated by the pressure gradients; Table 1). Consequently, we used the average water content and assumed constant velocity over the length of the column. Errors due to this assumption are presumed small because the column is short and pressure gradients were smaller than 1. Furthermore, *De Smedt and Wierenga* [1978], *Porro et al*. [1993], and *Selim et al*. [1977] found that despite nonuniform water content distributions, BTCs of solutes moving through unsaturated porous media under steady water flux conditions can be predicted using an average water content and an average dispersion coefficient.

4. Results

Results of our experiments show that breakthrough curves of NaCl exhibit earlier initial arrival and a higher degree of tailing under unsaturated flow conditions than under fully saturated conditions (Figure 2). Such behavior was quantified by analyzing initial and mean solute arrival and spread and skewness of the BTCs. To indicate the initial arrival of NaCl, an initial breakthrough pore volume (IBPV) was defined as the fraction of a pore volume eluted when the effluent concentration reaches 1% of the influent concentration. A plot of IBPV versus water content (Figure 3) shows that similar to β, the IBPV is lower under unsaturated conditions and tends to decrease as water content decreases.

The pore water velocities obtained from NaCl mean arrival times were in good agreement with the measured pore water velocities (determined from the column cross-sectional area, volumetric flow rates, and water contents), with an averaged error <3%. The deviations were all attributed to experimental error in water content measurements. As a result, the effective water contents were used for the remaining analysis of the data.

Generally, it can be observed in Table 1 that the variance for the BTCs tends to increase with decreasing water content. The variances of the BTCs also tend to increase with velocity for water contents above 20% by volume. Note that second and higher central moments for the slower saturated experiment (run NC 23; Table 1) were excluded because of incomplete data acquisition of the BTC. Although no correlation is observed between BTC variance and pressure gradients in the column, the higher variances for lower water contents (<20% by volume) are generally associated with smaller pressure gradients because pressure gradients tend to decrease as water

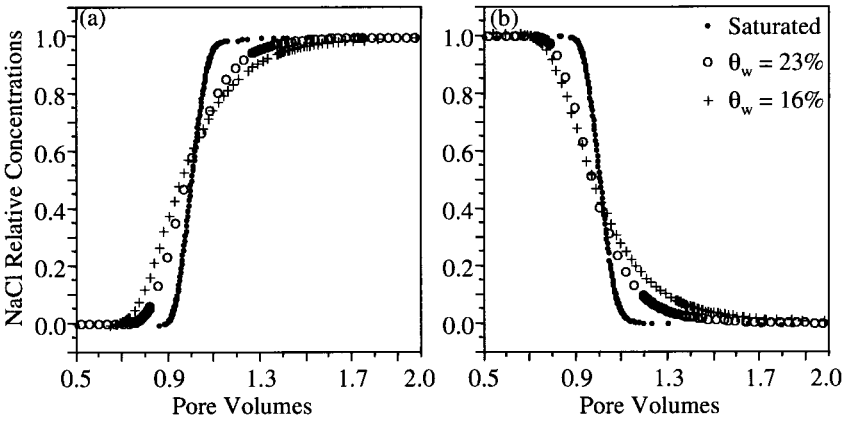

Figure 2. (a) Arrival and (b) elution limbs of experimental breakthrough curves for NaCl column effluent under different flow conditions.

content decreases. It is therefore assumed that spatial variations in soil-water tension do not affect velocity variations to a great extent in these experiments.

The BTCs tend to reflect a slight decrease in skewness with decreasing water contents below 26% (Table 1). The skewness of the BTCs also seems to increase slightly with increasing pore water velocity. These trends, however, are associated with a large uncertainty because the calculations may involve large errors [*Fahim and Wakao*, 1982; *Leij and Dane*, 1992; *Sardin et al*., 1991]. Greater BTC skewness with increasing velocity has also been reported by *Rao et al*. [1980b] for transport experiments conducted with saturated aggregates. They attribute this behavior to slower mixing resulting from preferential flow and slower rate-limited processes.

Attempts to estimate the transport parameters using the moments calculated from our experimental data were not successful [*Padilla*, 1998]. It appears that this method is highly sensitive to the accuracy of the moment estimate; a slight error (especially, in the skewness) can lead to erroneous parameter values.

The transport parameters obtained from CXTFIT by fitting the experimental results to the CDE equilibrium and nonequilibrium (MIM) models are given in Table 2. For saturated conditions both the CDE equilibrium and MIM models adequately simulate the BTCs. For unsaturated flow conditions, however, the coefficients of determination (r^2) for the regression of observed versus fitted concentrations [*Toride et al*., 1995] show that the MIM yields a better overall fit (r^2 ranges between 0.999 and 1.000) than the CDE equilibrium model (r^2 ranges from 0.994 to 1.000). Plots of measured versus simulated relative concentrations show that MIM-simulated C/C_0 fall on a 45° line, whereas those from the CDE equilibrium model are scattered about this line (Figure 4). This suggests that the relative concentrations (C/C_0) measured under unsaturated flow conditions were better represented by the MIM-simulated C/C_0 values than those from the CDE equilibrium model. In addition, a plot of residuals shows that the MIM model provides a better description of the solute early arrival and breakthrough tailing for unsaturated conditions than the CDE equilibrium model (Figure 5). Small standard deviations of the fitted pore water velocities, and their excellent agreement (>97%) with those obtained from the first-moment analysis and experimental measurement, indicate that both models are able to predict correctly the mean travel time of the BTCs. Although the models yield similar fitted dispersion coefficients for the saturated cases, the CDE equilibrium model yields higher values for unsaturated flow conditions than does the MIM model (Figure 6). In general, both models indicate that dispersion tends to increase as velocity increases and as water content decreases (Figure 6). Also, the MIM model values of β for unsaturated flow conditions decrease with decreasing water content (Figure 3). Similar to these results, *Griffioen et al*. [1998] indicate that mobile water fractions reported for unsaturated porous media range between 0.6 and 1 and tend to increase as water content increases. Furthermore, it was observed that under unsaturated conditions, β tends to increase slightly with increasing pore water velocity above 23% water content but decreases with increasing velocity for lower water contents. Although somewhat scattered, the results suggest that the fitted α values tend to increase with water content and pore water velocity for unsaturated conditions (Figure 7). Figure 8 shows the means and associated standard deviations (shown in error bars) of the fitted parameters as a function of water content. The standard deviations suggest that the dispersion coefficient is the most variable parameter, whereas α is the least variable.

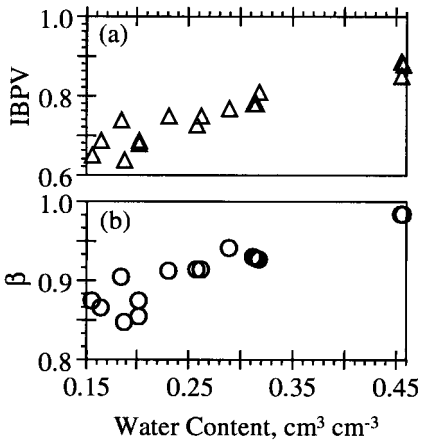

Figure 3. (a) Initial breakthrough pore volumes (IBPV) and (b) mobile water fraction β dependency on water contents.

5. Discussion

For solute transport under fully saturated flow conditions our experiments show that BTCs conform to the CDE solution, suggesting that the Fickian regime has been established.

Table 2. Results of the CXTFIT Parameter Optimization Model

	CDE Equilibrium Model		MIM Model			
Run	v, cm min^{-1}	D, cm^2 min^{-1}	v, cm min^{-1}	D, cm^2 min^{-1}	$\theta_m\theta^{-1}$, cm^3 cm^{-3}	α, min$^{-1} \times 10^{-3}$
Saturated						
NC 20	0.126	0.0042	0.126	0.0038	0.99	1.582
NC 21	0.126	0.0043	0.126	0.0038	0.99	1.172
NC 23	0.032	0.0014	0.032	0.0011	0.99	0.126
Unsaturated						
NaCl 1	0.184	0.0275	0.183	0.0110	0.93	1.944
NaCl 2	0.188	0.0281	0.187	0.0117	0.94	1.917
NaCl 3	0.183	0.0265	0.182	0.0081	0.93	1.869
NaCl 4	0.215	0.1052	0.213	0.0314	0.86	1.932
NaCl 5	0.166	0.0818	0.164	0.0240	0.85	1.326
NaCl 6	0.107	0.0502	0.106	0.0161	0.87	0.649
NaCl 7	0.078	0.0376	0.077	0.0132	0.88	0.372
NaCl 8	0.143	0.0605	0.143	0.0224	0.88	1.443
NaCl 9	0.195	0.0416	0.196	0.0145	0.92	1.886
NaCl 10	0.185	0.0443	0.186	0.0193	0.92	1.647
NaCl 12	0.095	0.0279	0.095	0.0111	0.91	0.564
NaCl 21	0.207	0.0360	0.208	0.0155	0.95	1.168
NaCl 22	0.197	0.0546	0.197	0.0216	0.92	1.717

CDE is convection-dispersion equation.

Conversely, our experiments of solute transport under unsaturated flow conditions reveal that the BTCs exhibit early initial arrival and long tailing, indicating that transport processes still remain at the pre-Fickian stage. These results appear to support the conjecture by *Yeh* [1998] that as a sand column becomes unsaturated, the number of flow paths decreases and velocity variations increase. Consequently, a plume moving in an unsaturated medium must travel a greater distance to attain complete mixing and to reach the Fickian regime than one in a saturated medium. These results are also consistent with findings of recent stochastic analysis of solute transport in large-scale heterogeneous vadose zones, which show that as

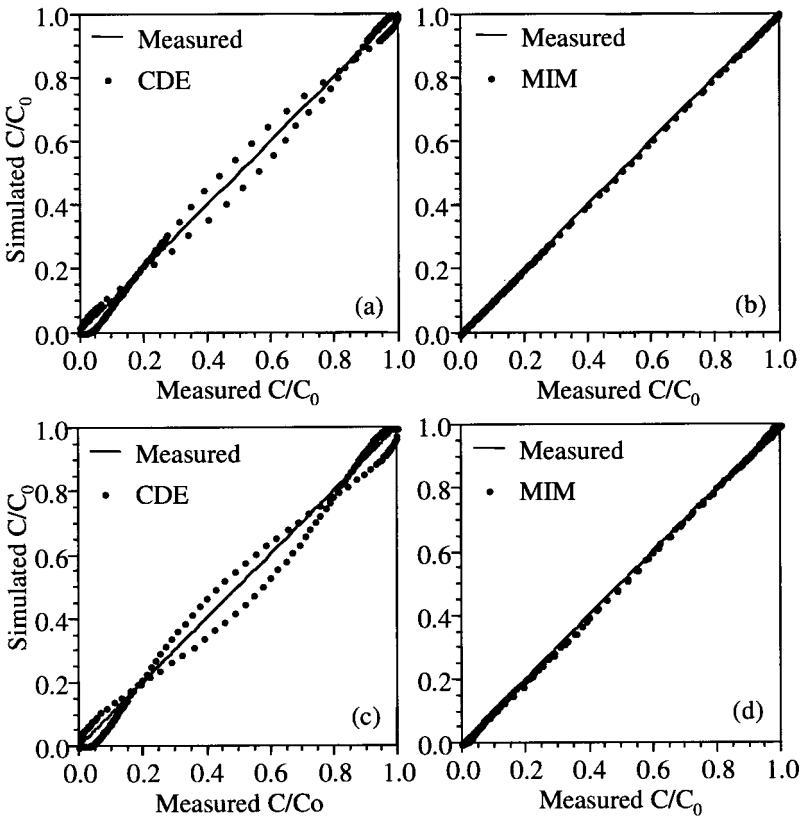

Figure 4. Measured versus simulated relative concentration using the (a) convection-dispersion equation (CDE) equilibrium and (b) mobile-immobile model (MIM) models for 18% water content and the (c) CDE equilibrium and (d) MIM models for 32% water content.

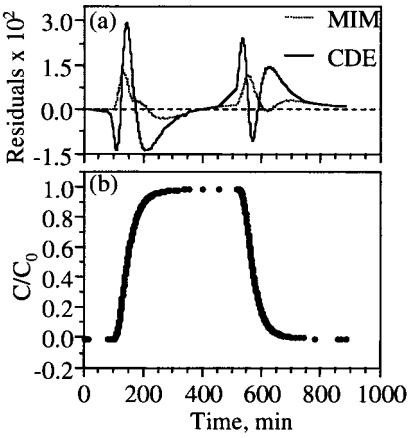

Figure 5. (a) Residuals from the MIM and CDE equilibrium models for (b) a NaCl breakthrough curve obtained at 18% water content.

the vadose zone becomes drier and more heterogeneous, the ensemble mean plume becomes highly skewed, and Fick's law no longer applies [*Harter and Yeh*, 1996].

To describe the non-Fickian behavior (early initial arrival and long tailing of BTCs) in stratified aquifers, a modified convection-dispersion equation has been proposed by several researchers [e.g., *Gelhar et al*., 1979; *Matheron and de Marsily*, 1980]. This equation includes higher-order spatial and temporal derivatives of concentration in addition to the dispersion and convection terms in the CDE. While the convection term represents the movement of a tracer due to the average velocity over the heterogeneous aquifer, the dispersion term captures the effect of velocity deviations due to stratification and mixing among layers. The higher-order temporal/spatial derivative terms then define the slow release of solutes entrapped in low-permeability beds in the aquifer during the pre-Fickian regime. These researchers further suggested that to allow the solute migration to reach the Fickian regime, a solute plume must travel over distances much greater than the thickness of stratification such that the effect of velocity variations due to stratification is balanced by local transverse dispersion among layers. *Matheron and de Marsily* [1980] further demonstrated that the Fickian regime can be reached over a short distance if the direction of groundwater flow is at an angle to the stratification so that large transverse mixing between layers is created. Results of all these studies simply suggest that a better mixing is the key to the development of the Fickian dispersion process.

Although the above-mentioned theories were developed to explain effects of large-scale heterogeneity, the same course of reasoning applies to the effects of pore-scale heterogeneity, manifested in results of our laboratory-scale experiments. It is therefore postulated that the above-mentioned modified convection-dispersion equation and the MIM model are conceptually similar. In other words the high and low conductive layers in the stratified aquifer correspond to the mobile and immobile regions of the MIM, respectively, and the transverse mixing across layers is then analogous to the local mixing or the mass transfer between the mobile and immobile waters. The MIM is thus considered to be an appropriate model for describing the pre-Fickian behavior of a solute plume at the column-scale tracer experiments.

It is important to point out that in contrast to our results, some laboratory tracer experiments in undisturbed soil columns have demonstrated earlier initial arrival and greater tailing of BTCs for saturated than for unsaturated flow conditions [*Gaber et al*., 1995; *Seyfried and Rao*, 1987]. This difference can be attributed to the difference in pore-size distribution of porous media. In a matrix with a highly skewed pore size distribution (such as a medium embedded with macropores, cracks, and aggregates), the distribution of solute velocity under fully saturated conditions is likely to be highly skewed as water moves rapidly through these features and slowly in the soil matrix. This skewed velocity distribution thus induces early initial breakthrough and greater BTC tailing and asymmetry. As water content decreases from saturation, these macropores drain first, and water flows through a less skewed pore-size distribution with a smaller mean value. Consequently, the distribution of flow velocity becomes less skewed, the velocity variations decrease, and the asymmetry of the BTC is reduced as the medium desaturates [*Seyfried and Rao*, 1987]. On the other hand, in a medium with a less skewed pore size distribution (such as the uniformly packed sand column used in this study) the velocity distribution under fully saturated conditions is expected to be less skewed and to show less tailing. Therefore solute breakthroughs in fully saturated homogeneous media conform to the Fickian behavior. As the medium desaturates, however, flow takes place in fewer flow channels, and velocity variations become greater. Consequently, as reflected in our experiments, BTCs exhibit earlier initial arrival and

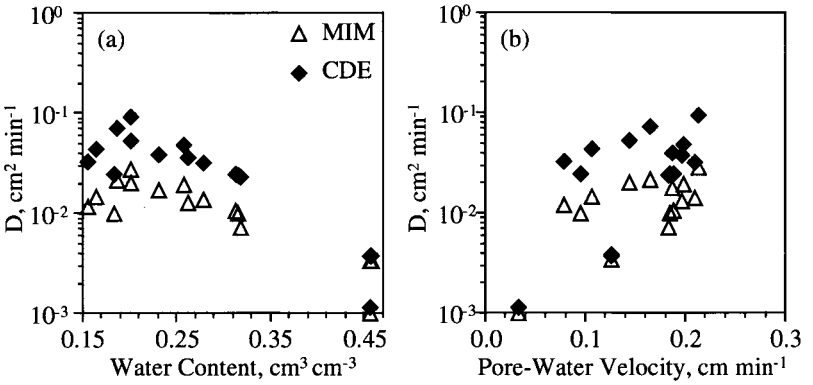

Figure 6. Fitted dispersion coefficient for the MIM and CDE equilibrium models as a function of (a) water content and (b) pore water velocity.

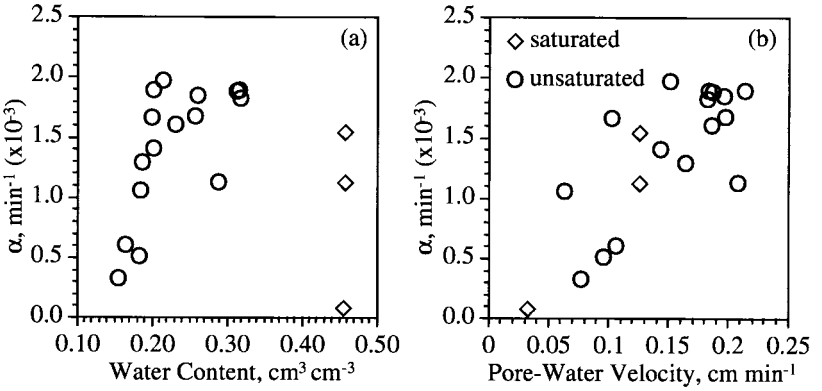

Figure 7. Influence of (a) water content and (b) pore water velocity on the MIM first-order mass transfer coefficient α.

greater tailing, thus becoming less symmetric with decreasing water content.

Although the MIM model adequately reproduced the less symmetric BTC observed under unsaturated conditions, the MIM model parameters are obtained by optimization, and unique solutions may not be obtained because the parameters are often correlated [*Bajracharya and Barry*, 1997; *Koch and Flühler*, 1993]. Our analysis, however, indicates that the parameter values are within realistic estimates. For instance, the excellent agreement between fitted and measured pore water velocities suggests that the model is able to predict correctly the mean velocity of the solute. Furthermore, the MIM-fitted β and α parameters obtained from our BTCs fall within the range of many published estimates [*Griffioen et al.*, 1998]. We also want to point out that although the CDE does not correctly describe the NaCl initial arrival and BTC tailing under unsaturated conditions, the dispersion coefficients estimated using the CDE equilibrium model (one-parameter optimization) yield similar trends as those estimated from the MIM model (Figure 6).

The dispersion term in (3a) is primarily influenced by molecular diffusion, fluid velocity, and medium characteristics [*Bear*, 1972]. Molecular diffusion under unsaturated flow conditions accounts for <6% of the mobile dispersion coefficients in our experiments and becomes less important as water content decreases (due to lower τ_w) and pore water velocity increases. The dependence of the dispersion coefficient on velocity has been well documented for saturated and unsaturated flow conditions [*Bear*, 1972; *De Smedt and Wierenga*, 1984; *Khan and Jury*, 1990] and is attributable to greater velocity variations at higher pore water velocities. In addition, our results show that the fitted dispersion coefficients are inversely related to average water contents and tend to increase as water contents decrease (Figure 6). Although the fitted dispersion coefficients did not show a strong relationship with pore water velocity ($r^2 = 0.30$), they showed a strong relationship with the ratio of the mobile water velocity to average mobile water content (Figure 9) given by an empirical power law:

$$D_m = \frac{D_h}{\beta} = \frac{D - D_w\tau_w}{\beta} \approx \eta\left(\frac{v_m}{\theta_m}\right)^n = \frac{\eta}{\theta_m^n}\, v_m^n = \xi_w(\theta_m) v_m^n, \tag{11}$$

where n is an empirical constant and $\xi_w(\theta_m)$ is saturation-dependent dispersivity. This relationship applies to the fitted dispersion coefficients from both MIM and CDE equilibrium models. Best fit values for n and η are 1.50 and 0.022, respec-

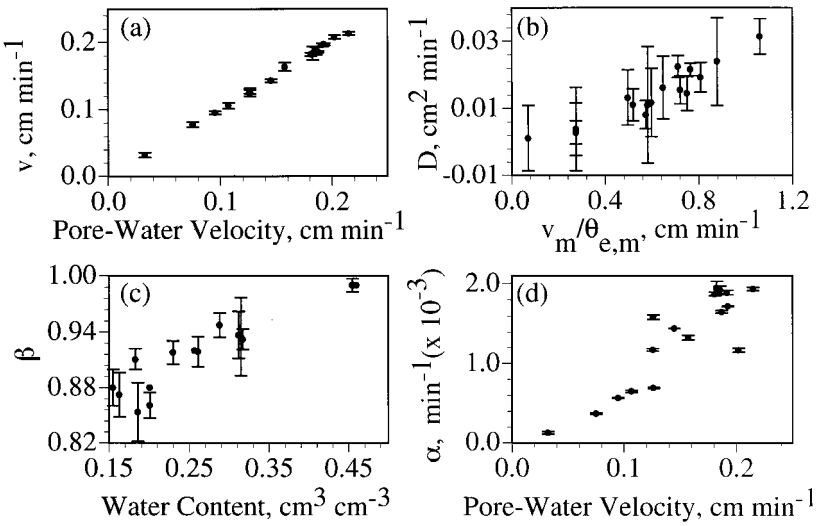

Figure 8. Means and standard deviations of MIM model parameters: (a) pore water velocity, (b) dispersion coefficient, (c) mobile water fraction, and (d) mass transfer coefficient.

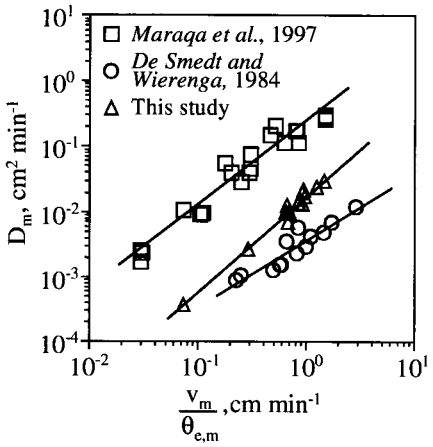

Figure 9. Log-log relationships between solute dispersion coefficient and the ratio of mobile velocity to water content.

tively, for the MIM model ($r^2 = 0.98$) and 1.99 and 0.085 for the CDE equilibrium model ($r^2 = 0.94$). Our proposed power law relationship (equation (11)) suggests that dispersivity is not only a characteristic of the porous medium but depends also on water content. Under saturated flow conditions, $\xi_w(\theta_m)$ is a constant and (11) reduces in form to the classic expression for the dispersion coefficient (equation (2)). For unsaturated flow conditions the inverse relationship between the dispersion coefficient and water content in (11) further suggests that the saturation-dependent dispersivity increases as water content decreases. Physically, this can be attributed to a smaller number of flow channels, more tortuous and smaller flow paths, and greater small-scale variations in water content as the medium desaturates. According to *Bear* [1972], the constant n is assumed to fall between 1 and 2, depending on the role played by transverse (perpendicular to flow) molecular diffusion. In pore channel systems in which mixing results from the combined effect of velocity distribution and transverse molecular diffusion, n is close to 2. Where mixing occurs only at junctions connecting pore channels, however, n is near 1. When applying the MIM model to describe our experimental data, n is 1.5, and solute mixing appears to occur from the combined effect of the different mechanisms. Other reported data for different porous media show similar relationships between dispersion and the ratio of mobile pore water velocity to water content (Figure 9) and yield similar values of n (1.1 and 1.3 for *De Smedt and Wierenga* [1984] and *Maraqa et al*. [1997], respectively).

Our results are also consistent with previous findings that relate dispersivity to particle size. In our analysis the lowest dispersivity constant ($\eta = 0.004$) was obtained for the medium used by *De Smedt and Wierenga* [1984] of which the particle diameter ranges from 88 to 125 μm. An intermediate value ($\eta = 0.022$) was obtained for our sand (diameter range 53–425 μm), and the highest value ($\eta = 0.26$) was obtained for the coarser media (diameter range 250–500 μm [*Maraqa et al*., 1997]). In accordance with other investigations [*Harleman and Rumer*, 1963; *Rose and Passioura*, 1971] the data show that dispersive properties of the media increase as the particle size distribution increases.

The mobile water fraction obtained from fitting experimental data to the MIM model shows that β is lower for unsaturated flow conditions and tends to decrease with water content (Figure 3). Lower β with decreasing water content is attributed to faster initial movement of the solute as it travels through a decreasing number of faster flow paths. As a result, β values are related to the initial arrival of the solute. In fact, *Gaudet et al*. [1977] and *Selim and Ma* [1995] observed that the mobile water fraction parameter affects the time of initial appearance of the solute. Similar trends between IBPV and β as a function of water content in our experiments (Figure 3) also indicate that the values of the two parameters are closely related. In general, the initial breakthrough time increases as β increases. A regression analysis of IBPV versus β yields an excellent linear relationship ($\beta = 0.55$ IBPV + 0.50 and $r^2 = 0.94$), suggesting β can be used to predict the time of initial arrival of a solute given average water contents and velocities. Moreover, IBPV can be used to estimate values of β for solute transport predictions in unsaturated sand. An explicit expression for IBPV was developed in terms of experimentally determined systems parameters. This expression (IBPV = 1.09 $\theta_w^{0.27}$ and $r^2 = 0.92$) indicates that IBPV is mainly a function of water content and, because of the linear relationship between IBPV and β, further supports that β is a function of water content. Although it is recognized that the above given empirical relationships are limited to porous media similar to that used in our experiments, such relationships point out that MIM model parameters for conservative tracers are related to water content. Similar to other hydraulic and transport parameters (e.g., saturated hydraulic conductivity, soil water retention characteristics, dispersivity), however, the mobile and immobile water fractions depend on the medium [*Bajracharya and Barry*, 1997] and must be evaluated for different porous media.

Variations of β with water content and pore water velocity appear to reflect the system's degree of departure from the Fickian regime. For instance, greater β with increasing pore water velocity at higher water contents (above 23%) denotes a more uniform velocity field and suggests that transport conditions are closer to the Fickian regime. At lower water contents, however, decreasing β values with increasing velocity suggest greater velocity variations and the possible existence of preferential flow paths. Lower β values may therefore indicate a lower degree of solute mixing and a greater departure from the Fickian regime.

The extent of solute mixing can also be assessed from the fitted α values. The results presented herein show that although somewhat scattered, α tends to increase with water content and pore water velocity (Figure 7). Qualitatively, it can be speculated that greater water contents may also result in a greater contact area for solute exchange between the mobile and immobile regions and a shorter, less tortuous path within the immobile region. Consequently, solute mixing occurs at a faster rate at high water contents. Lower water contents, on the other hand, may result in limited contact areas and longer, more tortuous diffusion paths. Solute exchange between water regions therefore occurs at a slower rate, and the solute must travel longer distances or times to achieve complete mixing.

Greater velocities enhance mass transfer rates by causing faster mixing between the two regions [*van Genuchten and Wierenga*, 1977; *De Smedt and Wierenga*, 1984]. This mass transfer mechanism is analogous to the transverse dispersion in stratified aquifers as analyzed by *Matheron and de Marsily* [1980], i.e., when mean groundwater flow is at an angle to the stratification, greater transverse dispersion occurs at high velocities. These results indicate that higher pore water velocities and water contents enhance solute mixing so that complete

spatial averaging is approached. In other words, the greater α values at higher water contents and velocities may indicate that the system will reach the Fickian regime faster.

From the above discussion it becomes clear that although solute transport in unsaturated porous media is likely under pre-Fickian conditions, better solute mixing can enhance the development of Fickian conditions. Results from recent transport experiments under unsaturated conditions using trichloroethene (TCE) [*Padilla*, 1998] further support this inference. These experiments show that BTCs for TCE are generally more symmetric than those for NaCl under the same unsaturated condition, suggesting that gas phase diffusion of TCE can enhance solute mixing. *Padilla* [1998] therefore concluded that TCE transport in unsaturated porous media attains Fickian conditions at shorter distances than transport of nonreactive solutes.

Finally, we want to point out that while the MIM model appears to provide a good fit to our data, it may not be an adequate representation of the underlying physics of solute transport processes in unsaturated porous media. Experimental and numerical studies of laboratory and field-scale heterogeneous aquifers have shown solute breakthrough with multiple peaks at early times of the transport process [*Sudicky et al*., 1983; *Wheat and Dawe*, 1988]. These results suggest that, for some heterogeneous porous media, solute mixing between preferential flow paths and the rest of porous media is limited, particularly during the very early stages of the pre-Fickian regime. Under these circumstances, the MIM model would not be appropriate. It is also logical to postulate that the necessity of using the MIM model may diminish as the solute travels over great distances. This is because solute concentrations in the mobile and immobile zones may approach equilibrium (i.e., the Fickian regime) due to better mixing. Due to nonuniform distribution of mobile and immobile water zones, the fitted parameters of the MIM model may vary with the length of the experiment until the Fickian regime is fully established. While the above discussion is speculative, we hope it will lead to more experiments in the future to investigate the evolution of the solute spread at different distances under unsaturated conditions.

6. Conclusions

Analysis of the BTCs indicates that solute transport in homogeneous porous media is subjected to non-Fickian conditions under unsaturated flow, but it conforms to Fickian conditions under saturated flow. In general, lower water content results in greater velocity variations and less mixing of the solute. As a result, solutes must travel longer distances to achieve better mixing and complete spatial averaging so that Fickian conditions can be attained. It is therefore concluded that greater deviations from the Fickian regime occur as water content decreases. This behavior, however, may vary with the pore size distribution of the soil.

In view of the inadequacy of the classical CDE to describe the movement of solutes under pre-Fickian conditions the MIM model was needed to reproduce the BTCs obtained under unsaturated flow conditions. It is found that the MIM parameter values (dispersivity, mass transfer coefficient, and mobile water fraction) in unsaturated porous media vary with water content. Furthermore, it is shown that dispersivity is not only a function of porous media but also inversely proportional to water content.

Acknowledgments. Funding for this research was provided by the National Institute of Environmental Health Sciences (grant ES04949) and the U.S. Geological Survey (grant 1434-92-G-2258). The authors are grateful to R. Bruant for his thorough review of the manuscript and extremely good comments and suggestions and J. Smith for his contributions to the experimental setup. We would also like to thank R. S. Mansell and the anonymous reviewer who provided insightful and constructive comments and suggestions for this manuscript. We are indebted to L. Abriola and the Associate Editor J. Bahr for their assistance in improving the manuscript.

References

Armstrong, J. E., E. O. Frind, and R. D. Mcclellan, Nonequilibrium mass transfer between the vapor, aqueous, and solid phases in unsaturated soils during vapor extraction, *Water Resour. Res*., *30*, 355–368, 1994.

Bajracharya, K., and D. A. Barry, Nonequilibrium solute transport parameters and their physical significance: Numerical and experimental results, *J. Contam. Hydrol*., *24*, 185–204, 1997.

Bear, J., *Dynamics of Fluids in Porous Media*, 764 pp., Elsevier, New York, 1972.

Bond, W. J., and P. J. Wierenga, Immobile water during solute transport in unsaturated sand columns, *Water Resour. Res*., *26*, 2475–2481, 1990.

Brunauer, S., P. H. Emmett, and E. Teller, Adsorption of gases in multimolecular layers, *J. Am. Chem. Soc*., *60*, 309–319, 1938.

Burdine, N. T., Relative permeability calculations from pore size distribution data, *Trans. Am. Inst. Min. Metall. Pet. Eng*., *198*, 71–77, 1953.

Coats, K. H., and B. D. Smith, Dead-end pore volume and dispersion in porous media, *SPEJ Soc. Pet. Eng. J*., *4*, 73–84, 1964.

Danielson, R. E., and P. L. Sutherland, Porosity, in *Methods of Soil Analysis*, *Agronomy*, vol. 9, 2nd ed., edited by A. Klute, pp. 443–461, Am. Soc. of Agron., Madison, Wis., 1986.

De Smedt, F., and P. J. Wierenga, Solute transfer through soil with nonuniform water content, *Soil Sci. Soc. Am. J*., *42*, 7–10, 1978.

De Smedt, F., and P. J. Wierenga, Solute transfer through columns of glass beads, *Water Resour. Res*., *20*, 225–232, 1984.

De Smedt, F., F. Wauters, and J. Sevilla, Study of tracer movement through unsaturated sand, *J. Hydrol*., *85*, 169–181, 1986.

Fahim, M. A., and N. Wakao, Parameter estimation from tracer response measurements, *Chem. Eng. J. Lausanne*, *25*, 1–8, 1982.

Fischer, H. B., E. J. List, R. C. Y. Koh, J. Imberger, and N. H. Brooks, *Mixing in Inland and Coastal Waters*, 483 pp., Academic, San Diego, Calif., 1979.

Gaber, H. M., W. P. Inskeep, S. D. Comfort, and J. M. Wraith, Nonequilibrium transport of atrazine through large intact soil cores, *Soil Sci. Soc. Am. J*., *59*, 60–67, 1995.

Gaudet, J. P., H. Jégat, G. Vachaud, and P. J. Wierenga, Solute transfer, with exchange between mobile and stagnant water, through unsaturated sand, *Soil Sci. Soc. Am. J*., *41*, 665–671, 1977.

Gelhar, L. W., *Stochastic Subsurface Hydrology*, 390 pp., Prentice-Hall, Englewood Cliffs, N. J., 1993.

Gelhar, L. W., A. L. Gutjahr, and R. L. Naff, Stochastic analysis of macrodispersion in a stratified aquifer, *Water Resour. Res*., *15*, 1387–1397, 1979.

Griffioen, J. W., D. A. Barry, and J.-Y. Parlange, Interpretation of two-region model parameters, *Water Resour. Res*., *34*, 373–384, 1998.

Harleman, D. R. F., and R. R. Rumer, Longitudinal and lateral dispersion in an isotropic porous medium, *J. Fluid Mech*., *16*, 385–394, 1963.

Harter, T., and T.-C. J. Yeh, Stochastic analysis of solute transport in heterogeneous, variably saturated soils, *Water Resour. Res*., *32*, 1585–1595, 1996.

Khan, A. U., and W. A. Jury, A laboratory study of the dispersion scale effect in column outflow experiments, *J. Contam. Hydrol*., *5*, 119–131, 1990.

Klute, A., Water retention: Laboratory methods, in *Methods of Soil Analysis*, *Agronomy*, vol. 9, 2nd ed., edited by A. Klute, pp. 635–662, Am. Soc. of Agron., Madison, Wis., 1986.

Koch, S., and H. Flühler, Solute transport in aggregated porous media: Comparing model independent and dependent parameter estimation, *Water Air Soil Pollut*., *68*, 275–289, 1993.

Leij, F. J., and J. H. Dane, Moment method applied to solute transport with binary and ternary exchange, *Soil Sci. Soc. Am. J*., *56*, 667–674, 1992.

Ma, L., and H. M. Selim, Tortuosity, mean residence time, and deformation of tritium breakthroughs from soil columns, *Soil Sci. Soc. Am. J.*, *58*, 1076–1085, 1994.

Maraqa, M. A., R. B. Wallace, and T. C. Voice, Effects of degree of water saturation on dispersivity and immobile water in sandy soil columns, *J. Contam. Hydrol.*, *25*, 199–218, 1997.

Matheron, G., and G. de Marsily, Is transport in porous media always diffusive? A counterexample, *Water Resour. Res.*, *16*, 901–917, 1980.

Matsubayashi, U., L. P. Devkota, and F. Takagi, Characteristics of the dispersion coefficient in miscible displacement through a glass beads medium, *J. Hydrol.*, *192*, 51–64, 1997.

Nielsen, D. R., M. T. van Genuchten, and J. W. Biggar, Water flow and solute transport processes in the unsaturated zone, *Water Resour. Res.*, *22*, 89–108, 1986.

Padilla, I. Y., Transport of nonreactive and volatile solutes in unsaturated porous media under wetting and draining conditions, Ph.D. dissertation, 311 pp., Univ. of Ariz., Tucson, 1998.

Porro, I., P. J. Wierenga, and R. G. Hills, Solute transport through large uniform and layered soil columns, *Water Resour. Res.*, *29*, 1321–1330, 1993.

Rao, P. S., R. E. Jessup, D. E. Rolston, J. M. Davidson, and D. P. Kilcrease, Experimental and mathematical description of nonadsorbed solute transfer by diffusion in spherical aggregates, *Soil Sci. Soc. Am. J.*, *44*, 684–688, 1980a.

Rao, P. S. C., D. E. Rolston, R. E. Jessup, and J. M. Davidson, Solute transport in aggregated porous media: Theoretical and experimental evaluation, *Soil Sci. Soc. Am. J.*, *44*, 1139–1145, 1980b.

Rose, D. A., and J. B. Passioura, The analysis of experiments on hydrodynamic dispersion, *Soil Sci.*, *111*, 252–257, 1971.

Sardin, M., D. Schweich, F. J. Leij, and M. T. van Genuchten, Modeling the nonequilibrium transport of linearly interacting solutes in porous media: A review, *Water Resour. Res.*, *27*, 2287–2307, 1991.

Selim, H. M., and L. Ma, Transport of reactive solutes in soils: A modified two region approach, *Soil Sci. Soc. Am. J.*, *59*, 75–82, 1995.

Selim, H. M., J. M. Davidson, and P. S. C. Rao, Transport of reactive solutes through multilayered soils, *Soil Sci. Soc. Am. J.*, *41*, 3–10, 1977.

Seyfried, M. S., and P. S. C. Rao, Solute transport in undisturbed columns of an aggregated tropical soil: Preferential flow effects, *Soil Sci. Soc. Am. J.*, *51*, 1434–1444, 1987.

Sudicky, E. A., J. A. Cherry, and E. O. Frind, Migration of contaminants in groundwater at a landfill: A case study, *J. Hydrol.*, *63*, 81–108, 1983.

Toride, N., F. J. Leij, and M. T. van Genuchten, The CXTFIT code for estimating transport parameters from laboratory or field tracer experiments, *Rep. 137*, 121 pp., U.S. Salinity Lab., Riverside, Calif., 1995.

Valocchi, A. J., Validity of the local equilibrium assumption for modeling sorbing solute transport through homogeneous soils, *Water Resour. Res.*, *21*, 808–820, 1985.

van Genuchten, M. T., A closed-form equation for predicting the hydraulic conductivity of unsaturated soils, *Soil Sci. Soc. Am. J.*, *44*, 892–898, 1980.

van Genuchten, M. T., and J. C. Parker, Boundary conditions for displacement experiments through short laboratory soil columns, *Soil Sci. Soc. Am. J.*, *48*, 703–708, 1984.

van Genuchten, M. T., and P. J. Wierenga, Mass transfer studies in sorbing porous media, I, Analytical solutions, *Soil Sci. Soc. Am. J.*, *40*, 473–480, 1976.

van Genuchten, M. T., and P. J. Wierenga, Mass transfer studies in sorbing porous media, II, Experimental evaluation with tritium (^3H_2O), *Soil Sci. Soc. Am. J.*, *41*, 272–277, 1977.

Welty, J. R., C. E. Wicks, and R. E. Wilson, *Fundamentals of Momentum, Heat, and Mass Transfer*, 3rd ed., 803 pp., John Wiley, New York, 1984.

Wheat, M. R., and R. A. Dawe, Transverse dispersion in slug-mode chemical EOR processes in stratified porous media, *SPE Reservoir Eng.*, *285*, 466–478, 1988.

Wierenga, P. J., and M. T. van Genuchten, Solute transport through small and large unsaturated soil columns, *Ground Water*, *27*, 35–42, 1989.

Yeh, T.-C. J., Scale issues of heterogeneity in vadose-zone hydrology, in *Scale Dependence and Scale Invariance in Hydrology*, edited by G. Sposito, pp. 423, Cambridge Univ. Press, New York, 1998.

M. H. Conklin, I. Y. Padilla, and T.-C. J. Yeh, Department of Hydrology and Water Resources, University of Arizona, P.O. Box 210011, Tucson, AZ 85721-0011. (ybiem@mac.hwr.arizona.edu)

(Received December 8, 1997; revised May 17, 1999;
accepted May 25, 1999.)